Title

Rad54 Functions as a Heteroduplex DNA Pump Modulated by Its DNA Substrates and Rad51 during D Loop Formation

Journal

Molecular Cell, 53(3)

ISSN

1097-2765

Authors

Wright, William Douglass
Heyer, Wolf-Dietrich

Publication Date

2014-02-01

DOI

10.1016/j.molcel.2013.12.027

Peer reviewed

Published in final edited form as:
Mol Cell. 2014 February 6; 53(3): 420–432. doi:10.1016/j.molcel.2013.12.027.

Rad54 functions as a Heteroduplex DNA Pump Modulated by Its DNA Substrates and Rad51 during D-loop Formation in Homologous Recombination

William Douglass Wright[1,*] and **Wolf-Dietrich Heyer**[1,2,*]

[1] Department of Microbiology & Molecular Genetics, University of California, Davis, Davis CA 95616-8665, USA

[2] Department of Molecular & Cellular Biology, University of California, Davis, Davis CA 95616-8665, USA

Summary

The displacement loop (D-loop) is the product of homology search and DNA strand invasion, constituting a central intermediate in homologous recombination (HR). In eukaryotes, Rad51 recombinase is assisted in D-loop formation by the Rad54 motor protein. Curiously, Rad54 also disrupts D-loops. How these opposing activities are coordinated toward productive recombination is unknown. Moreover, a seemingly disparate function Rad54 is removal of Rad51 from heteroduplex DNA (hDNA) to allow HR-associated DNA synthesis. Here, we uncover novel features of D-loop formation/dissociation dynamics, employing Rad51 filaments formed on ssDNAs that mimic physiological length and structure of *in vivo* substrates. The Rad54 motor is activated by Rad51 bound to synapsed DNAs and guided by a newly discovered single-stranded DNA binding domain. We present a unified model where Rad54 acts as an hDNA pump, which drives D-loop formation while simultaneously removing Rad51 from hDNA, consolidating both ATP-dependent activities of Rad54 into a single mechanistic step.

Introduction

Homologous recombination (HR) is active in every domain of life and vitally contributes to genomic maintenance. A central intermediate in HR is a joint DNA molecule called the displacement loop (D-loop). This structure forms when a DNA strand exchange protein such as Rad51 forms a filament on ssDNA, which then executes homology search and DNA strand invasion into a homologous dsDNA donor (**Figure 1A**). D-loop formation is a vital regulatory point in HR (Heyer et al., 2010) because it marks the stage when the ssDNA sequence has successfully located a homologous DNA reference sequence and has formed heteroduplex DNA (hDNA). If the 3′ end of the invading ssDNA is in hDNA, it is competent for extension by a DNA polymerase, facilitating the recovery of lost sequence information. Hence, *in vitro* reconstituted D-loop reactions have been a central assay for the

*Corresponding author; (530) 752-3001 wdheyer@ucdavis.edu.

Additional experimental procedures are described in the supplement.

study of the mechanisms of HR proteins for decades (Shibata et al., 1979). Significant gaps in our knowledge of the basic reaction mechanisms persist to this day.

The prototypical DNA strand exchange protein is RecA from *E. coli*. RecA forms D-loops *in vitro* autonomously, *i.e.* in the absence of other proteins (Shibata et al., 1979). In contrast, *S. cerevisiae* Rad51 requires a protein cofactor to form D-loops such as Rad54 (Petukhova et al., 1998). This difference is likely related to the differences in their ATPase activities and regulation of DNA binding by nucleotide cofactor (discussed in Heyer et al. 2006). Like RecA, Rad51 is capable of promoting a three-strand exchange reaction between circular ssDNA and linear dsDNA without Rad54 (Sung, 1994). The critical difference in the D-loop reaction is that the homology located within the donor is internal, away from an end, requiring strand *invasion* to displace the complementary strand. This mirrors the *in vivo* situation of a resected DSB invading an intact chromosome. There are several competing models on the mechanism of Rad54 in Rad51-mediated D-loop formation that have yet to be resolved, as discussed below (Ceballos and Heyer, 2011; Heyer et al., 2006; Mazin et al., 2010; Tan et al., 2003). The mitotic HR defect of a *rad54*Δ mutant in *S. cerevisiae* is essentially as severe as *rad51*Δ in assays requiring strand invasion (Heyer et al., 2006), highlighting the requirement for Rad54 and the tight partnership of the Rad51 and Rad54 activities *in vivo*.

Rad54 is a member of the Swi2/Snf2 family of dsDNA translocases and remodelers of protein-dsDNA complexes (Hopfner et al., 2012). The most fundamental activity of the enzyme is dsDNA-dependent ATPase (Swagemakers et al., 1998), which fuels processive and rapid (~300 bp/sec) translocation on dsDNA (Amitani et al., 2006). Genetic data corroborate that the ATPase activity of Rad54 is essential for HR, as Walker A box mutations affecting ATP hydrolysis cause essentially the same DNA damage sensitivity as the gene deletion (Clever et al., 1999; Petukhova et al., 1999). Next to the well-conserved core dsDNA-binding motor domain, Snf2 family proteins have additional domains that regulate motor activity by mechanistically coupling the ATPase domain with the substrate in the remodeling reaction (Hopfner et al., 2012). Often this regulation includes enhancement of ATPase/remodeling activity when the regulatory domain interacts with its target. In Rad54, this regulatory domain appears to be within the N-terminal region, which interacts with Rad51 in a species-specific fashion (Mazin et al., 2000; Petukhova et al., 1999; Raschle et al., 2004). In fact, Rad54 specifically remodels Rad51:dsDNA filaments and dissociates Rad51 from dsDNA (Solinger et al., 2002). The Rad51-dsDNA substrate stimulates the Rad54 ATPase up to six-fold over protein-free dsDNA (Kiianitsa et al., 2002). Rad54 ATPase activity is also stimulated 3-4 fold over dsDNA by DNA junctions containing ssDNA in addition to dsDNA (Mazina et al., 2007). Hence, the fundamental dsDNA-dependent ATPase activity of Rad54 is modulated by interaction with Rad51 and DNA substrates, but it is unclear how this is integrated in the formation of D-loops.

Detailed biochemical and *in vivo* studies addressing the function of Rad54 in HR have revealed independent mechanisms by which Rad54 might support D-loop formation by Rad51. First, Rad54 associates with and stabilizes Rad51:ssDNA filaments, whereby Rad54 is delivered to the target dsDNA, where it can exert its ATPase activity (Mazin et al., 2000; Van Komen et al., 2000). Rad51:ssDNA filament stabilization is independent of the Rad54

ATPase *in vitro* and *in vivo* (Mazin et al., 2003; Wolner and Peterson, 2005), and therefore is unlikely to be the critical activity. Second, Rad54, similar to other Snf2-like protein complexes, is capable of remodeling nucleosomes in an ATP-dependent fashion (Alexeev et al., 2003). While one can easily envision how nucleosome expulsion would support homology search, Rad54 is essential for Rad51-mediated D-loop formation on protein-free duplex DNA *in vitro*. Hence, while it is possible that this activity supports HR *in vivo*, it does not explain why Rad54 is required for Rad51-mediated D-loop formation. Third, it has been suggested that Rad54 translocation on dsDNA aids in the homology search by sliding target DNA past the Rad51:ssDNA filament (Ristic et al., 2001). This model posits a fundamental difference between the homology search catalyzed by RecA, which does not engage a Rad54-like factor and Rad51. Fourth, Rad54 and its ATPase activity are required for Rad51-mediated strand invasion to intertwine the invading ssDNA with its complement in donor dsDNA to produce a D-loop. Rad54 was proposed to mediate topological opening of donor dsDNA by inducing DNA supercoils (Tan et al., 1999; Van Komen et al., 2000). Fifth, Rad54 has been shown to dissociate Rad51 from the hDNA after DNA strand exchange allowing access to the invading 3′-end by a DNA polymerase to prime HR-associated DNA synthesis (Li and Heyer, 2009; Solinger et al., 2002). It is puzzling that the Rad54 ATPase is envisioned to act at three seemingly separate stages of HR, presynapsis (homology search), synapsis (D-loop formation) and post-synapsis (Rad51-dsDNA dissociation).

D-loops formed by the bacterial RecA protein with short ssDNA fragments under ATP hydrolysis conditions quickly dissociate, initially described as the D-loop cycle (Shibata et al., 1982). Reminiscent of these *in vitro* reactions with RecA, human and yeast Rad54 were demonstrated to disrupt short RAD51-mediated D-loops *in vitro* (Bugreev et al., 2007). This activity has been suggested to contribute to the SDSA pathway of HR (Bugreev et al., 2007) but the physiological relevance of Rad54-mediated D-loop disruption is unclear.

In this study, the activities of the budding yeast Rad54 protein in both D-loop formation and dissociation are examined in the context of DNA substrates designed to more closely mimic the physiological context for Rad51 filament formation. These ssDNA substrates are much longer than typically used in conventional *in vitro* assays and more closely reflect the physiological extent of resection. In addition, they contain dsDNA regions flanking the homologous ssDNA to mimic 5′-resected DSB ends. Surprisingly, D-loops formed with these substrates are much more stable to Rad54-mediated disruption. Contrary to expectation, we find that a homologous free ssDNA end is not required for D-loop formation. Moreover, we show that one ssDNA molecule may invade multiple dsDNA targets. DNA supercoiling, a prerequisite for RecA-mediated D-loop formation, is not required for the Rad51/Rad54-dependent reaction. These data are synthesized into a model that consolidates the critical ATP-dependent activities of Rad54, D-loop formation in conjunction with Rad51, and Rad51 displacement from hDNA, into a single mechanistic step where Rad54 acts as an hDNA pump. The model predicts an additional ssDNA binding site on Rad54 that provides orientation for the Rad54 hDNA pump, which was identified in the regulatory N-terminal region of Rad54 from yeast and humans.

Results

Rad54 catalyzes D-loop formation and disruption

The D-loop reaction (**Fig. 1A**) with *S. cerevisiae* Rad51, Rad54, and RPA proteins was optimized experimentally (**Fig. S1**). The *S. cerevisiae* Rad51/Rad54 system was employed because the reaction is robust under the physiological magnesium-ATP conditions needed to study Rad54. **Figure 1B** shows the time course of D-loop product levels using a 100 nt ssDNA paired with supercoiled plasmid DNA (denoted *100*::sc). A short, fully homologous ssDNA oligonucleotide such as this is typical for most *in vitro* studies using the D-loop assay. D-loops increase with time after plasmid/Rad54 addition for 6-10 minutes, level off, and then decrease with time thereafter. At the bulk level, formation and dissociation of D-loops likely occur simultaneously, and the observance of net formation and dissociation phases may reflect that Rad51:ssDNA filaments become inactive over time. To establish that Rad54 is responsible for D-loop dissociation, a *197*::sc reaction was shifted to 37° C, because at this temperature Rad54, but not Rad51, looses activity within 5-10 min (Van Komen et al., 2002). If Rad54 is responsible for the D-loop disruption, incubation at 37° C should specifically inhibit the dissociation phase. Indeed, as shown in **Figure 1C**, while shifting from 23° to 30° C did not affect the dissociation phase (both slopes are −1.2 % D-loop/min), shifting to 37° C significantly decreased the dissociation phase. Moreover, Rad54 disrupts deproteinized *100*::sc D-loops (data not shown). These results implicate Rad54 in disruption of native D-loops and are consistent with observations using human RAD54 (Bugreev et al., 2007).

Physiological pre-synaptic ssDNA substrates promote the formation of stable D-loops

In vivo, the ssDNA revealed by 5′ to 3′ resection of a DSB end is hundreds of nucleotides long (Zhu et al., 2008). One consequence of the traditional use of relatively short ssDNA substrates *in vitro* for D-loop formation is that the potential length of hDNA is limited. In addition, D-loops formed with short ssDNAs lack branchpoints in the D-loops where the hDNA region ends and the non-incorporated part of the invading ssDNA exits. *In vivo*, the rest of the broken chromosome arm always forms such a branchpoint, where there is double- or single-stranded DNA exiting the hDNA formed in the D-loop (see **Fig. 7**).

To investigate possible differences in D-loop formation and dissociation dynamics as a consequence of the length and structure of the invading DNA used for Rad51 filament formation, a series of ssDNA substrates of different homology lengths were produced (**Fig. 2A**). The time courses of D-loop formation by these substrates were determined. As shown in **Figure 2B,C**, when the length of fully homologous ssDNA substrates is increased in the range of 65 to 1,201 nt, peak D-loop yields dramatically increase while the dissociation phase of the reaction (15' to 40') is attenuated (see **Table S1** for rates of formation and dissociation of each substrate). The longest ssDNA tested, 1,201 nt, completely lacks a dissociation phase. These time courses were compared to identical sequence substrates that possess 5′ dsDNA regions (‘tails’), meant to mimic the tailed ssDNA formed by DNA end resection *in vivo* (**Fig. 2B**). Surprisingly, the kinetic profiles of these dsDNA-tailed substrates looked dramatically different from their fully single-stranded, homology length counterparts. ssDNAs with dsDNA regions showed significantly less dissociation compared

to their non-tailed counterparts, even after normalization to differences in peak D-loop levels (*i.e.* normalizing to % of peak level lost per minute; **Table S1**). The dissociation phase is eliminated at a shorter length in 5′- 98ds substrates (see 98ds-*197*), while *607*, a substrate without flanking duplex DNA, still has unstable joint molecules (**Fig. 2C**). This suggests that the dsDNA region blocks Rad54-mediated D-loop disruption. These patterns were reconfirmed using a series of ssDNA and donor dsDNA substrates of identical lengths but a different sequence (**Fig. S2**), eliminating the possibility of sequence-specific effects.

Long Rad51 filaments can invade multiple target duplex DNAs

With the use of ssDNA substrates 402 nt or longer discrete, slow-migrating D-loop species appeared (**Figs. 2B,D, S2**). Their electrophoretic migration suggests that these species contain one ssDNA molecule that has formed hDNA with multiple plasmid DNA molecules (**Fig. S3A**). While multiple invasion (MI) events involving two donor DNAs were not surprising for ssDNAs with two homologous ends, they were unexpected for the tailed substrates that contain only a single homologous end. Similarly, MIs events involving more than two donor DNAs were unexpected. The 5′ duplex tails impart stability to MI species formed with 402 or 607 nt of homology (**Figs. 2D, S2B**). A subsequent invasion event might be expected to produce a shorter hDNA tract than the primary one. This is consistent with the observation that 402 and 607 nt homology MI species have pronounced dissociation phases (**Table S1**), as do the primary (and only) invasion species of D-loops formed with short ssDNAs (**Figs. 1, 2, 3**). The *607*::sc reactions have stable primary invasions but unstable MIs. In contrast, at 1,201 nt homology, 30-40 % of the invading ssDNAs are in MIs, and all species show very little disruption, regardless of the presence of 5′ duplex tails (**Fig. 2D,E**). Taken together, these time course data suggest that increasing homology length and the presence of 5′ dsDNA are both factors that stabilize D-loops to Rad54-mediated disruption.

Terminal heterologies protect D-loops from Rad54-mediated disruption on both sides of the homology

Having established that a 5′ dsDNA region on the invading nucleoprotein filament attenuates Rad54-mediated D-loop dissociation, experiments were designed to test whether the terminal heterologous region had to be double-stranded, and whether it had to flank the 5′ side of the homologous ssDNA region. A short homology length was chosen, 65 nts, to allow for robust Rad54-mediated disruption. The *65* nt homology was flanked with different combinations on the 5′ and/or 3′ sides with either double or single-stranded heterologies. Reaction time courses were performed to test the effect of these appendages on Rad54-mediated D-loop formation/disruption phases (**Fig. 3 A,B**). As expected, the elimination of homologous free ssDNA ends with the addition of terminal heterologies progressively lowers the initial rates of the reactions (**Table S1)**. Interestingly, the heterologous regions on either side of the homology attenuate the dissociation phase (15 to 40 minutes) of Rad51/Rad54 D-loop reactions (**Table S1**). **Figure 3A** shows five DNA substrates with heterologies on one side of the 65 nt homology. dsDNA heterologies consistently had a greater effect at blocking the disruption as judged by the greater accumulation of D-loops compared to their ssDNA heterology counterparts (**Fig. 3A**; compare ss35-*65* with ds35-*65*;

65-35ss with *65*-35ds). **Figure 3B** presents substrates where heterologies are present on both sides of the homology. When the heterologies are both ssDNA, D-loop levels are barely detectable (< 0.5%). However, when the heterology on one or both sides is double-stranded, D-loops accumulate (**Fig. 3B**) without evidence of a dissociation phase (**Table S1**). This suggests that dsDNA character at the hDNA branchpoint stabilizes D-loops to a greater extent than ssDNA, in this case allowing D-loops to accumulate by attenuating the reverse reaction, D-loop disruption. Further, the stabilizing effects of terminal heterologies/dsDNA are independent of the polarity of the invading strand. Finally, homologous ssDNA ends stimulate but are not required for Rad51/Rad54 catalyzed D-loop formation. These results support a mechanism of HR-mediated gap repair with strand invasion by a Rad51 filament in the absence of a DNA end.

Rad51/Rad54 catalyze strand invasion in the absence of DNA supercoiling

When considering D-loop formation and stability, the topological status of the donor dsDNA is important because DNA supercoiling stimulates the homologous pairing reactions promoted by both Rad51/Rad54 and RecA (Shibata et al., 1979; Van Komen et al., 2000). For each 10.4 bp hDNA generated in the D-loop, one negative supercoils is dissipated releasing its stored energy. The D-loops resulting from the incorporation of long ssDNAs have an electrophoretic mobility consistent with the total relaxation of donor supercoils (**Figs. 2B, S3B**).

RecA absolutely requires negatively supercoiled donor dsDNA for D-loop formation, while Rad51 and Rad54 can catalyze D-loop formation in relaxed (yet covalently-closed) plasmid DNA (Van Komen et al., 2000). In such a closed substrate, Rad54 translocation was envisioned to create local supercoiling and strand opening that facilitated Rad51 filaments to perform strand invasion (Tan et al., 1999; Van Komen et al., 2000). However, it is unknown whether Rad51/Rad54 can promote hDNA formation by strand invasion into linear dsDNA, where supercoils generated by Rad54 will dissipate. To test this, a dsDNA donor was created by linearization of the normal scDNA with *Bsa*I. In the resulting linear dsDNA, the ssDNA-homologous region is flanked by long heterologous regions requiring strand invasion into the interior of the linear donor dsDNA (**Fig. 4A)**. As expected, RecA incorporated about 44 % of ds98-*607* ssDNA into D-loops in the supercoiled plasmid reaction, but no D-loops were detected with the linear dsDNA donor (**Fig. 4B**). Surprisingly, Rad51/Rad54 formed about 20 % D-loops when linear dsDNA was the donor (**Fig. 4D**). Rad54 did not stimulate RecA in D-loop assays using either linear dsDNA or scDNA (data not shown).

It is unlikely that Rad54 binding to linear dsDNA creates domains within which supercoils are produced, since this would require, at minimum, two Rad54 translocation units (12-24 Rad54 monomers, if the complex is a hexamer or double hexamer) acting on the same molecule of dsDNA. As Rad54 is titrated into 98ds-*607*::lin reactions (standard 21 μM bp, 7 nM molecules dsDNA donor), near-maximal D-loop levels are already achieved by about 20 nM Rad54, corresponding to only about three monomers per linear dsDNA molecule (**Fig. S1D**). If supercoil generation were the means that Rad54 stimulated linear D-loop formation, the optimal Rad54 concentration in the 7 nM linear dsDNA reaction would be

expected to be at least 84 nM (12 monomers/dsDNA). Therefore, another mechanistic model is required to explain how Rad54 is able to input the energy necessary to promote hDNA formation.

Linear D-loops are in a different realm of stability because they are not stabilized by negatively-supercoiled donor dsDNA. Reflecting this, linear D-loops are much less thermostable than D-loops in supercoiled donors (**Fig. S3C,D**). In addition, the shortest substrate to support linear D-loop formation had 197 nt homology, whereas as little as 65 nt supported the supercoiled reaction (**Figs. 2C, 4C**). In this sensitized context, the stabilizing effects of terminal heterologies have much greater influence on D-loop levels. A particularly good demonstration of this comes from comparison of ds98-*197* and *197* ssDNAs on linear and supercoiled substrates (**Fig. 4C**). Without a duplex tail, the *197*::lin D-loops are unstable, peaking at just 2 % and then dissociating. With 5′ dsDNA present, the ds98-*197*::lin reaction yields 12 % D-loops, without appreciable dissociation.

Next, we determined how terminal heterologies affected longer homology substrates when paired with the standard supercoiled substrate or with linear dsDNA. Heterologous regions were added to the 607 nt substrate, which was paired with both linear and supercoiled DNAs (**Fig. 4D**). When paired with supercoiled DNA, heterologies had similar effects on the kinetics of D-loop formation as seen for the 65 nt homology series. The availability of homologous ssDNA ends favors faster D-loop formation, dominating the kinetics of the formation phase of the reaction. In contrast, the terminal heterologous regions had the opposite effect on the formation phase of linear D-loops. The 0 min to 3 min slope for structures with dual heterologies is about twice (~6 %/min) the slope of fully homologous *607*::lin (3.4 %/min). The stability imparted by the terminal heterologies now dominate, allowing these substrates to accumulate at a faster rate when paired with a linear dsDNA donor. These data indicate that even for substrates where there is no observable net dissociation of D-loops in time course experiments, Rad54-mediated D-loop dissociation can occur.

Mapping hDNA formation using a site-specific hDNA generation assay

The use of long ssDNAs substrates, analogous to those formed *in vivo*, adds further complexity to the D-loop reaction because the extent of hDNA generation possible is limited by the topological status of the dsDNA donor. When hDNA is generated in a D-loop, the supercoils in the dsDNA are dissipated, one supercoil per about 10.4 bp hDNA formed. Based on the average supercoil density of plasmids purified from *E. coli* (−0.07), the 3 kb plasmid donor used in this study contains about 20 negative supercoils, and can therefore accommodate about 210 bp of heteroduplex maximum. Therefore, ssDNA that is significantly longer than 210 nt homology will not be fully assimilated into hDNA and ssDNA will protrude from the D-loop structure.

To understand better where hDNA forms with respect to the invading strand polarity, a site-specific hDNA detection assay was devised. In this assay, only invading ssDNA incorporated into hDNA (dsDNA) can be cleaved by restriction enzymes, so site-specific hDNA formation can be monitored by the cleavage efficiency of restriction sites in the invading ssDNA (**Fig. 5A**). A homology length of 607 nts was chosen to allow measurement

of the polarity of the strand invasions with respect to the invading strand. The two restriction sites are relatively close to the ends, 5′- *Mlu*I and 3′- *Bst*XI (with respect to the invading strand polarity) are 134 and 111 nt in from the ends, respectively. Importantly, these sites are 362 nt apart on the invading strand, which is larger than the maximum 210 bp hDNA allowed in the 3 kb plasmid substrate. Therefore, this assay reports on the kinetics of incorporation of a 5′-proximal site *versus* a 3′-proximal site into hDNA; this distinction can be made because *both* sites cannot be incorporated in the same supercoiled donor plasmid.

The analysis of fully homologous *607* D-loops is shown in **Figure 5B**. Both 5′- *Mlu*I and 3′- *Bst*XI restriction sites are made cleavable in a time-dependent manner after initiation of the D-loop reaction with Rad54/dsDNA, reflecting their incorporation into hDNA. Both ssDNA ends are incorporated into hDNA, with a modest preference for the 3′ end-proximal *Bst*XI site. The preference for 3′- *Bst*XI cleavage to 5′- *Mlu*I is about 2.5-fold at the initial 1 min. time point (32.8 ± 2.2 to 13.3 ± 1.6 %) and 1.5-fold (47.6 ± 1.2 to 32.5 ± 2.4 %) when D-loops peak at 13 min. The same 3′ end invasion preference is also evident for 98-*607* linear D-loops (**Fig. S4D-F**). A preference for incorporation of the 3′ end into hDNA likely reflects the biological necessity to incorporate this end into hDNA in order to prime recombination-associated DNA synthesis.

Since *Mlu*I and *Bst*XI are mutually exclusive for cleavage, the sum of cleavages at the two restriction sites (dotted red line) in comparison to the total level of D-loops (solid blue) is informative. For both *607* and ds98-*607* substrates, the sum of cleavages at either end of the homology equals the total D-loop level at every time point examined (**Fig. 5B,C**). This has certain implications: 1) Little hDNA forms solely within the middle of the invading molecules because of the preference for the ssDNA ends to form hDNA. If D-loops formed exclusively within the 362 nt region containing neither restriction site, it would not be cleaved and D-loop levels would exceed the sum of cleavages at *Bst*XI and *Mlu*I sites. 2) The MI species contain either *Bst*XI or *Mlu*I in hDNA but rarely both. MIs could conceivably contain both sites in hDNA since two plasmids molecules are engaged; however, this would predict that the total cleavages would be in excess of the total D-loops, which is not observed. This may reflect that secondary invasions contain shorter tracks of hDNA. The level of cleavage never decreases for one site and increase for the other, suggesting that large-scale branch migration in these joint molecules does not readily occur after the initial hDNA formation, consistent with the lack of a dissociation phase in time courses of D-loops formed with these substrates.

The ssDNA end preference was analyzed using an additional restriction site in the middle of the invading strand (*Bts*CI, **Fig. 5D**). Adding heterologous duplex regions to either side of *607* blocks the preference for that end to be incorporated into hDNA. 98ds-*607*-ds78, a substrate with heterologies on both ends, has virtually no site preference. These data suggest that hDNA formation can proceed in either direction in D-loop formation, either 3′ to 5′ or 5′ to 3′ with respect to the invading strand, with a preference (but not requirement) to start at a DNA end.

The question remains: How does Rad54 promote hDNA formation with respect to the Rad51 filament—is lateral association sufficient (*i.e.* Rad54 only contacts the contiguous Rad51

filament) or does Rad54 have to assist from a filament end? If Rad54 requires a filament terminus to promote hDNA formation, then sub-saturating amounts of Rad51 should form hDNA faster because the filaments will be discontinuous and have more ends for Rad54 to contact in hDNA formation. D-loop reactions were performed where Rad51 filaments were assembled on ds98-*607* DNA to varying degrees of saturation (**Fig. S4A**; full saturation is 1 Rad51 per 3 nt/bp). Consistent with the prediction that Rad54 stimulates hDNA formation from filament ends, subsaturating Rad51 filaments formed higher levels of D-loops after 10 minutes than did saturating Rad51 filaments.

The hDNA digestion assay was used to measure internal 5′ *versus* 3′ hDNA incorporation of ds98-*607* as a function of Rad51 saturation. Both sites were incorporated into hDNA more efficiently at subsaturating Rad51 concentrations (**Fig. S4B**). Rad51 concentration did not change the relative incorporation of the two sites, as the fully homologous 3′ end-proximal *Bst*XI site was always favored 2-2.5 fold over the internal *Mlu*I site. The time needed for hDNA formation to reach completion was assessed by calculating the % final level of digestion already achieved at the first measurement (1 min). This speed of completion value decreases steadily with increasing Rad51 concentration (**Fig. S4C**). These results are consistent with Rad51 filament ends being the limiting substrate for Rad54-mediated hDNA generation, and Rad54 initiating heteroduplex formation at the termini of Rad51 filaments.

The N-terminal regulatory domain of Rad54 interacts specifically with ssDNA

We envisioned that Rad54 functions as an hDNA pump (elaborated below), and as such Rad54 complexes would not only have to interact with the dsDNA it translocates on, but also with the displaced strand in the form of ssDNA. This could be mediated through an ssDNA binding domain outside of the dsDNA-engaged core motor domain, which we sought to identify. The N-terminal domain of Rad54 is the best candidate, since it was already shown to interact with Rad51, which leads to stimulation of Rad54 activity (Kiianitsa et al., 2002). To test this possibility, Rad54 N-terminal fragments from both yeast (y54-N; amino acids 1-273) and human (h54-N, amino acids 1-155) were purified (**Fig. 6A,B**) and tested for DNA binding activity by electrophoretic mobility shift assays (EMSA).

Yeast and human 54-N proteins both bound 3 kb dsDNA or ssDNA avidly (**Fig. 6C,F**), though the shift in the ssDNA was difficult to observe until high protein concentration. However, a strong preference for ssDNA binding was revealed under competitive conditions where both ssDNA and dsDNAs were present simultaneously (**Fig. 6C,F**). In this case, the dsDNA was not bound until the ssDNA binding was completely saturated. To further support this conclusion, 3 μM y54-N was pre-bound to 7.6 μM bp or nt dsDNA or ssDNA. y54-N bound up all dsDNA in the well, but was easily liberated by the addition of 3-6 μM ssDNA. In contrast, ssDNA-bound y54-N was not competed even with 15 μM dsDNA (**Fig. 6D**), demonstrating the strong ssDNA binding preference of this domain. Since the binding of ssDNA was difficult to quantify due to the subtle/smeared mobility shift, the ssDNA binding preference of y54-N was quantitatively reconfirmed with short 65 nt or bp DNAs that do not enter PAGE gels upon y54N binding (**Fig. S5A**). EMSA gels for y54-N and h54-N were transferred to membranes and blotted with yeast or human Rad54 antibodies to

confirm that the 54-N species were indeed responsible for the DNA binding activity and not a contaminant in the preparations (**Fig. S5B,C**).

In vivo, ssDNA is covered by RPA as soon as it is generated. Therefore, if the 54-N ssDNA binding is biologically relevant RPA should not interfere. This premise was tested by comparing the abilities of ssDNA and RPA-coated ssDNA (1 RPA trimer to 25 nt) to challenge pre-formed 54-N:dsDNA complexes (**Fig. 6E,G**). For both y54-N and h54-N, the efficiency with which protein-free *versus* cognate RPA-coated ssDNA liberated 54-N from dsDNA complexes was indistinguishable (**Fig. 6E,G**), suggesting that 54-N can either bind RPA-coated ssDNA or displace RPA effectively. Supporting the latter hypothesis, blotting of the h54-N EMSA gel and probing with RAD54 antibody reveals that the migration of the h54-N:ssDNA complexes is not affected by the presence of hRPA, while hRPA:ssDNA complexes have much slower electrophoretic mobility before h54-N binding (**Fig. 6G**). In summary, these data are consistent with a model where Rad54 complexes bind the displaced DNA strand through the N-terminal domain.

Discussion

The mechanism of Rad54 in Rad51-mediated D-loop formation

Based on the experiments presented here we arrive at the following important conclusions:

1. Rad54 supports Rad51-mediated D-loop formation with linear duplex DNA as target (**Fig. 4**) under conditions where it is unlikely that Rad54-induced global topological changes (Tan et al., 1999; Van Komen et al., 2000) are the key mechanism stimulating Rad51 in D-loop formation.
2. Our novel substrates allowed demonstration that terminal heterologies and/or long homology length that exceeds the capacity for hDNA formation increase D-loop formation approaching 90% product by eliminating D-loop dissociation by Rad54. These data suggest that specific structural elements of the D-loop with protruding DNA affect the Rad54 motor protein.
3. A key aspect is that hDNA formation begins at termini of Rad51:ssDNA filaments. Microscopic analysis has revealed that large Rad54 oligomers, presumably translocation units, associate with the termini of Rad51 filaments (Kiianitsa et al., 2006; Sanchez et al., 2013). Filament-terminal association on the invading ssDNA puts Rad54 in position to engage in translocation (hDNA pumping) upon the two nascent hDNA strands to promote their intertwining (see **Fig. 7**). Gaps in the Rad51 ssDNA filament provide more Rad51 filament termini for Rad54 to be also localized interstitially in Rad51:ssDNA filaments (Sanchez et al., 2013), explaining why subsaturating Rad51 filaments on ssDNA enhance D-loop formation (**Fig. S4**; (Van Komen et al., 2000)) compared to fully saturated conditions. As Rad54 is targeted to the pairing site *via* the Rad51:ssDNA filament, the Rad54 motor can engage on dsDNA to initiate translocation (hDNA pumping).
4. hDNA formation can initiate at interstitial sites in the Rad51:ssDNA filament as indicated by the observation that Rad51/Rad54 readily produce hDNA away from a homologous ssDNA end (**Figs. 3-5**). Though a 3′ end is preferred for hDNA

incorporation when available (**Fig. 5**), internal invasion events occur readily in gapped ssDNAs lacking homologous ends. In fact, hDNA formation away from ssDNA ends is so prevalent that MI species are produced, providing a mechanism for the formation of complex joint molecules *in vivo*. Multi-chromatid joint molecules were found in wild type cells and shown to accumulate in *sgs*1 mutants during meiosis (Oh et al., 2007). One class of such events is analogous to the MI species described here, suggesting that also *in vivo* a single long Rad51/Dmc1 filament may target two independent donor dsDNA molecules.

5. Another Rad54-stimulating factor in addition to Rad51 is the displaced DNA strand. Mazina and coworkers (Mazina et al., 2007) have demonstrated that ssDNA-containing branched joint molecules stimulate Rad54 ATPase activity. Here, the ssDNA binding domains of yeast and human Rad54 proteins is shown to lie within the N-terminal regions (**Fig. 6**), which also contains the Rad51 interaction domain (Raschle et al., 2004). A truncation mutant of Rad54 lacking the implicated N-terminal region, Rad54 (270-898), almost completely lacks ATPase activity (**Fig. S5E**), as does the equivalent N-terminal truncation of *Drosophila* Rad54 (Alexiadis et al., 2004).

We combine our data with previous findings into a novel hDNA pump model (**Fig. 7A**) that consolidates previously disparate results on the ATPase-dependent functions of Rad54 during D-loop formation and Rad51 dissociation from hDNA. We suggest that Rad54 acts as an hDNA pump, simultaneously forming hDNA and displacing Rad51, the motor activity being given directionality and stimulation by both Rad51 and the displaced strand. Rad54 pumps the invading strand and donor dsDNA in, and threads out hDNA and the displaced strand. In doing so, Rad54 effectively creates its substrate (double-stranded hDNA) for translocation just ahead of itself as the base pairs of nascent hDNA are united. Meanwhile, the N-terminal domain engages the ssDNA of the to-be-displaced strand in register, and either passively guides or actively transports the strand through the Rad54 complex, while the ssDNA also stimulates the pump activity. hDNA is cleared of Rad51 as it is generated, so that a DNA polymerase has immediate access to the 3′ end of the invading strand, if the end has been incorporated into heteroduplex.

Like Rad54, the well-characterized bacterial chromosomal DNA pump FtsK is also a DNA translocase but *not* a DNA helicase (Bigot et al., 2005). Rad54 and FtsK are also analogous in that they both induce supercoiling when translocating on dsDNA (Saleh et al., 2005; Tan et al., 1999; Van Komen et al., 2000). While FtsK action is oriented by the KOPS DNA sequence motif (Bigot et al., 2005), we envision that Rad54 translocation is oriented by the three-dimensional structure and architecture of hDNA junctions defined by Rad51 and the displaced strand in the D-loop, interacting with the newly discovered, conserved ssDNA binding domain in the N-terminus of Rad54.

Human RAD51 can form D-loops autonomously in the presence of calcium, which inhibits the RAD51 ATPase (Bugreev and Mazin, 2004). However, calcium is an unlikely *in vivo* cofactor and the calcium-supported reaction is still strongly stimulated by RAD54 (Mazina and Mazin, 2004). D-loops formed *in vitro* with the human proteins in magnesium

conditions are also completely RAD54-dependent (Sigurdsson et al., 2002). Hence, we suggest that also human RAD54 acts as an hDNA pump similar to yeast Rad54 (**Fig. 7A**).

Rad54 and D-loop disruption

Disruption of the D-loop is a required step for SDSA, the primary mechanism for HR-mediated DSB repair in somatic cells, and a mechanism of anti-recombination. A number of proteins have been proposed to specifically catalyze D-loop disruption, including Mph1 and Sgs1 in yeast, as well as RECQ1 and RTEL1 in mammals (reviewed in (Heyer et al., 2010)). Human RAD54 has also been implicated in D-loop disruption based on biochemical experiments (Bugreev et al., 2007). As shown here (**Fig. 1**), yeast Rad54 protein also promotes D-loop dissociation in the standard D-loop reactions. However, using substrates with more physiological features (length, DNA junctions; see **Fig. 7B**), D-loops accumulate to higher levels and dissociation of D-loops is diminished. Collectively, the data suggests that when the hDNA tract in a D-loop has reached sufficient length, and/or is stabilized by DNA junctions at the hDNA boundary, they are no longer susceptible to Rad54-mediated dissociation. Hence, this explains the need for other proteins to disrupt the D-loop intermediate in order to promote SDSA (Heyer et al., 2010). The model (**Fig. 7B**) also explains the curious observation of D-loop disruption by Rad54. *In vivo*, whether the HR substrate is a processed DSB end or a gapped ssDNA, there is always dsDNA present flanking the homology and therefore the D-loops formed will be resistant to Rad54-mediated disruption. Adding a dsDNA region to ssDNAs used for gene targeting increases their recombination frequency in CHO cells (Tsuchiya et al., 2008). This confirms that dsDNA flanking ssDNA homology is also a stabilizing factor *in vivo*, here explained by the resistance of these substrates to Rad54 disruption.

The observed D-loop disruption activity of Rad54 may be most relevant to short heteroduplex tracts that might form during the homology search when the Rad51 filament encounters homeologous donor DNA sequences. Indeed, net disruption of short 65 nt homology D-loops was observed, even when a dsDNA region was present on the invading ssDNA (**Fig. 3**). Disruption of such short hDNA tract D-loops by Rad54 could augment the homology search by quickly bypassing homeologous regions, which are especially plentiful in higher eukaryotes. In addition, D-loop dissociation activity may be relevant for events where ssDNA fragments, such as viral DNA or degradation products, would engage in HR.

In sum, using DNA substrates that better mimic those formed during HR *in vivo*, we have uncovered novel characteristics of the D-loop reaction. These data are interpreted in a model to explain how Rad54 translocation is coupled to D-loop formation and Rad51 turnover by acting as an hDNA pump. This model consolidates the seemingly disparate functions previously proposed for RAD54 in D-loop formation and Rad51 turnover into a single mechanistic step.

Experimental Procedures

ssDNA substrate production

Short structures—Short ssDNA containing substrates with individual strands 65 to 135 nt in length were prepared with synthetic oligonucleotides (PAGE-purified, Invitrogen). Structures, if containing dsDNA regions, were annealed and all DNAs were PAGE purified as described (Wright et al., 2011).

Long structures—Structures containing strands 197 nt or longer were obtained by manipulation of circular ssDNAs produced by ssDNA rescue from modified pBluescript KS- phagemids (see **Fig. S6**). First, the multiple cloning site (MCS) of this vector was expanded with two inserts (~75 bp) to introduce additional restriction sites on both the 5′ (*Sac*I/*Btg*I insert) and 3′ (*Xho*I/*Kpn*I insert) sides of the MCS (polarities are with respect to the rescued strand). Then, 197, 402, 607, and 1,201 nt of homology to either phiX174 (bps 5′ 2280 to 3′ 2084, 1879, 1674, or 1080; standard sequence) or the *S. cerevisiae RAD51* gene (ORF bps 5′ 198, 403, 608, or 1202 to 3′ position 3; alternative sequence) were cloned into the *Xba*I (5′) and *Hin*dIII (3′) sites of the MCS. PCR was used to add these cloning sites to the gene fragments as well as a *Pst*I site and an *Nco*I site immediately adjacent to the 5′ and 3′ sides of the fragments, respectively. Production of phagemid circular ssDNA from these vectors using M13K07 helper phage (NEB) was carried out according to the manufacturer′s instructions.

Long structures with full homology—To create a fully homologous ssDNA, short oligos (18-20 mers; 3-10 fold molar excess to circular ssDNA) were annealed to ~40-80 μg phagemid ssDNA in 1-1.5 ml (50 mM potassium acetate, 20 mM tris-acetate, 10 mM magnesium acetate, pH 7.9) at the 5′ and 3′ sides of the homology such that the *Pst*I and *Nco*I restriction sites were made double-stranded. *Pst*I and *Nco*I were added at 2 U/ μg phagemid ssDNA and digestion was carried out for 1 hour at 37 °C. The sequence and cut sites were designed such that when these sites are digested with both these enzymes the ssDNA liberated from the phagemid backbone is fully homologous to phiX174 (the alternative *RAD51* gene sequence has a 5′ non-homologous “G” after cleavage and is otherwise homologous to *RAD51*). The annealed oligonucleotides retain maximally six nt complimentary to the ssDNA product after cleavage, which are removed in the following purification procedure along with the phagemid backbone and other contaminants. Reactions are deproteinized with 0.6% SDS, 1 mg/ml proteinase K for 30 min at 45°C, then diluted into 15 ml TAE and concentrated in a 15 ml centrifugal filter device (Millipore) to ~200μl. This material is separated on a 4%, 10×10 cm TAE-PAGE gel at 100V for ~2 hr. Product bands are visualized by UV shadowing, excised, electroeluted from the gel slices into TAE buffer, then concentrated, as described (Wright et al., 2011).

Long structures with terminal heterologies—To add terminal heterologies to either side of the homologies, the procedure is the same as above except that oligonucleotides annealing/enzyme digestion is carried out using the engineered sites added in the expansion of the MCS (typically 5′*Sma*I, cutting 98 bp 5′ of the homology start and 3′ *Eco*72I, 78 bp past the homology). To make these regions double-stranded on the 5′ side, an additional 20-

mer oligonucleotide is annealed immediately adjacent to the start of the homology. After digestion, 2 μM dNTP mix and Klenow fragment exo- (at 1 U/ug phagemid DNA; NEB) are added for 10 min at 37°C to fill in from the 3′end of the 20-mer to the fragment end at the *Sma*I cleavage site, to create a 98 bp duplex region. To create 3′ duplex DNA, instead of a short cleavage oligonucleotide, a longer oligonucleotide is annealed for the cleavage step spanning from the 3′ end of the homologous region to past the *Eco*72I cleavage site.

dsDNA Donor Substrate Production

Homology donor plasmids were constructed by fusing the replication/selection-essential sequences of pBluescript, (bps 1160 to 2958) with 1201 bp segments of either phiX174 (bps 1080-2280) or the *RAD51* gene sequence (ORF bps 3-1,202). *Hin*dIII and *Xba*I sites were added to both fragments *via* PCR and cloning was completed using standard techniques to produce a 3kb plasmid. Large-scale plasmid preparations were produced by detergent lysis, followed by cesium chloride gradient centrifugation. Linear dsDNA was created by digestion of 50 μg plasmid donors with *Bsa*I. Digests were extracted twice with phenol/chloroform, once with chloroform, and ethanol precipitated.

Supplementary Material

Refer to Web version on PubMed Central for supplementary material.

Acknowledgments

We thank X.-P. Zhang for the y54-N expression plasmid, S. Kowalczykowski for RecA as well as helpful criticism, N. Hunter and M. Brinkmeyer for helpful comments on the manuscript, and K. Ehmsen, X. Li, and J. Liu for purifying proteins used in this study. WDW was supported by a dissertation fellowship from TRDRP (17DT-0178). This work was supported by grant GM58015 from the National Institutes of Health.

References

Alexeev A, Mazin A, Kowalczykowski SC. Rad54 protein possesses chromatin-remodeling activity stimulated by a Rad51-ssDNA nucleoprotein filament. Nature Struct Biol. 2003; 10:182–186. [PubMed: 12577053]

Alexiadis V, Lusser A, Kadonaga JT. A conserved N-terminal motif in Rad54 is important for chromatin remodeling and homologous strand pairing. J Biol Chem. 2004; 279:27824–27829. [PubMed: 15105430]

Amitani I, Baskin RJ, Kowalczykowski SC. Visualization of Rad54, a chromatin remodeling protein, translocating on single DNA molecules. Mol Cell. 2006; 23:143–148. [PubMed: 16818238]

Bianchi M, DasGupta C, Radding CM. Synapsis and the formation of paranemic joints by E. coli RecA protein. Cell. 1983; 34:931–939. [PubMed: 6313216]

Bigot S, Saleh OA, Lesterlin C, Pages C, El Karoui M, Dennis C, Grigoriev M, Allemand JF, Barre FX, Cornet F. KOPS: DNA motifs that control E. coli chromosome segregation by orienting the FtsK translocase. EMBO J. 2005; 24:3770–3780. [PubMed: 16211009]

Bugreev DV, Hanaoka F, Mazin AV. Rad54 dissociates homologous recombination intermediates by branch migration. Nature Struct Mol Biol. 2007; 14:746–753. [PubMed: 17660833]

Bugreev DV, Mazin AV. $Ca2^{+}$ activates human homologous recombination protein Rad51 by modulating its ATPase activity. Proc Natl Acad Sci USA. 2004; 101:9988–9993. [PubMed: 15226506]

Ceballos SJ, Heyer WD. Functions of the Snf2/Swi2 family Rad54 motor protein in homologous recombination. BBA. 2011; 1809:509–523. [PubMed: 21704205]

Clever B, Schmuckli-Maurer J, Sigrist M, Glassner B, Heyer W-D. Specific negative effects resulting from elevated levels of the recombinational repair protein Rad54p in Saccharomyces cerevisiae. Yeast. 1999; 15:721–740. [PubMed: 10398342]

Heyer WD, Ehmsen KT, Liu J. Regulation of homologous recombination in eukaryotes. Annu Rev Genet. 2010; 44:113–139. [PubMed: 20690856]

Heyer WD, Li X, Rolfsmeier M, Zhang XP. Rad54: the Swiss Army knife of homologous recombination? Nucleic Acids Res. 2006; 34:4115–4125. [PubMed: 16935872]

Hopfner KP, Gerhold CB, Lakomek K, Wollmann P. Swi2/Snf2 remodelers: hybrid views on hybrid molecular machines. Curr Opin Struct Biol. 2012; 22:225–233. [PubMed: 22445226]

Kiianitsa K, Solinger JA, Heyer WD. Rad54 protein exerts diverse modes of ATPase activity on duplex DNA partially and fully covered with Rad51 protein. J Biol Chem. 2002; 277:46205–46215. [PubMed: 12359723]

Kiianitsa K, Solinger JA, Heyer WD. Terminal association of Rad54 protein with the Rad51-dsDNA filament. Proc Natl Acad Sci USA. 2006; 103:9767–9772. [PubMed: 16785421]

Li X, Heyer WD. RAD54 controls access to the invading 3-OH end after RAD51-mediated DNA strand invasion in homologous recombination in Saccharomyces cerevisiae. Nucleic Acids Res. 2009; 37:638–646. [PubMed: 19074197]

Mazin AV, Alexeev AA, Kowalczykowski SC. A novel function of Rad54 protein - Stabilization of the Rad51 nucleoprotein filament. J Biol Chem. 2003; 278:14029–14036. [PubMed: 12566442]

Mazin AV, Bornarth CJ, Solinger JA, Heyer W-D, Kowalczykowski SC. Rad54 protein is targeted to pairing loci by the Rad51 nucleoprotein filament. Mol Cell. 2000; 6:583–592. [PubMed: 11030338]

Mazin AV, Mazina OM, Bugreev DV, Rossi MJ. Rad54, the motor of homologous recombination. DNA Repair. 2010; 9:286–302. [PubMed: 20089461]

Mazina OM, Mazin AW. Human Rad54 protein stimulates DNA strand exchange activity of hRad51 protein in the presence of $Ca2^{+}$. J Biol Chem. 2004; 279:52041–52051.

Mazina OM, Rossi MJ, Thomaa NH, Mazin AV. Interactions of human Rad54 protein with branched DNA molecules. J Biol Chem. 2007; 282:21068–21080. [PubMed: 17545145]

Oh SD, Lao JP, Hwang PYH, Taylor AF, Smith GR, Hunter N. BLM ortholog, Sgs1, prevents aberrant crossing-over by suppressing formation of multichromatid joint molecules. Cell. 2007; 130:259–272. [PubMed: 17662941]

Petukhova G, Stratton S, Sung P. Catalysis of homologous DNA pairing by yeast Rad51 and Rad54 proteins. Nature. 1998; 393:91–94. [PubMed: 9590697]

Petukhova G, Van Komen S, Vergano S, Klein H, Sung P. Yeast Rad54 promotes Rad51-dependent homologous DNA pairing via ATP hydrolysis-driven change in DNA double helix conformation. J Biol Chem. 1999; 274:29453–29462. [PubMed: 10506208]

Raschle M, Van Komen S, Chi P, Ellenbeger T, Sung P. Multiple interactions with the Rad51 recombinase govern the homologous recombination function of Rad54. J Biol Chem. 2004; 279:51973–51980. [PubMed: 15465810]

Ristic D, Wyman C, Paulusma C, Kanaar R. The architecture of the human Rad54-DNA complex provides evidence for protein translocation along DNA. Proc Natl Acad Sci USA. 2001; 98:8454–8460. [PubMed: 11459989]

Saleh OA, Bigot S, Barre FX, Allemand JF. Analysis of DNA supercoil induction by FtsK indicates translocation without groove-tracking. Nature Struct Mol Biol. 2005; 12:436–440. [PubMed: 15821742]

Sanchez H, Kertokalio A, van Rossum-Fikkert S, Kanaar R, Wyman C. Combined optical and topographic imaging reveals different arrangements of human RAD54 with presynaptic and postsynaptic RAD51-DNA filaments. Proc Natl Acad Scie USA. 2013; 110:11385–11390.

Shibata T, DasGupta C, Cunningham RP, Radding CM. Purified Escherichia coli recA protein catalyzes homologous pairing of superhelical DNA and single-stranded fragments. Proc Natl Acad Sci U S A. 1979; 76:1638–1642. [PubMed: 156361]

Shibata T, Ohtani T, Iwabuchi M, Ando T. D-loop cycle. A circular reaction sequence which comprises formation and dissociation of D-loops and inactivation and reactivation of superhelical

closed circular DNA promoted by recA protein of Escherichia coli. J Biol Chem. 1982; 257:13981–12986. [PubMed: 6754721]

Sigurdsson S, Van Komen S, Petukhova G, Sung P. Homologous DNA pairing by human recombination factors Rad51 and Rad54. J Biol Chem. 2002; 277:42790–42794. [PubMed: 12205100]

Solinger JA, Kiianitsa K, Heyer W-D. Rad54, a Swi2/Snf2-like recombinational repair protein, disassembles Rad51:dsDNA filaments. Mol Cell. 2002; 10:1175–1188. [PubMed: 12453424]

Sung P. Catalysis of ATP-dependent homologous DNA pairing and strand exchange by yeast RAD51 protein. Science. 1994; 265:1241–1243. [PubMed: 8066464]

Swagemakers SMA, Essers J, deWit J, Hoeijmakers JHJ, Kanaar R. The human Rad54 recombinational DNA repair protein is a double-stranded DNA-dependent ATPase. J Biol Chem. 1998; 273:28292–28297. [PubMed: 9774452]

Tan TLR, Essers J, Citterio E, Swagemakers SMA, de Wit J, Benson FE, Hoeijmakers JHJ, Kanaar R. Mouse Rad54 affects DNA conformation and DNA-damage-induced Rad51 foci formation. Curr Biol. 1999; 9:325–328. [PubMed: 10209103]

Tan TLR, Kanaar R, Wyman C. Rad54, a Jack of all trades in homologous recombination. DNA Repair. 2003; 2:787–794. [PubMed: 12826279]

Tsuchiya H, Uchiyama M, Hara K, Nakatsu Y, Tsuzuki T, Inoue H, Harashima H, Kamiya H. Improved gene correction efficiency with a tailed duplex DNA fragment. Biochemistry. 2008; 47:8754–8759. [PubMed: 18642931]

Van Komen S, Petukhova G, Sigurdsson S, Stratton S, Sung P. Superhelicity-driven homologous DNA pairing by yeast recombination factors Rad51 and Rad54. Mol Cell. 2000; 6:563–572. [PubMed: 11030336]

Van Komen S, Petukhova G, Sigurdsson S, Sung P. Functional cross-talk among Rad51, Rad54, and replication protein A in heteroduplex DNA joint formation. J Biol Chem. 2002; 277:43578–43587. [PubMed: 12226081]

Wolner B, Peterson CL. ATP-dependent and ATP-independent roles for the Rad54 chromatin remodeling enzyme during recombinational repair of a DNA double strand break. J Biol Chem. 2005; 280:10855–10860. [PubMed: 15653683]

Wright WD, Ehmsen KT, Heyer WD. Assays for structure-selective DNA endonucleases. Methods Mol Biol. 2011; 745:345–362. [PubMed: 21660704]

Zhu Z, Chung WH, Shim EY, Lee SE, Ira G. Sgs1 helicase and two nucleases Dna2 and Exo1 resect DNA double-strand break ends. Cell. 2008; 134:981–994. [PubMed: 18805091]

Highlights

- The structure of hDNA branchpoints modulate Rad54-mediated D-loop disruption
- Rad51/Rad54 promote formation of multiple invasion joint molecules
- The N-terminal, regulatory domain of Rad54 orients its motor activity
- Rad54 stimulates D-loop formation acting as a heteroduplex DNA pump

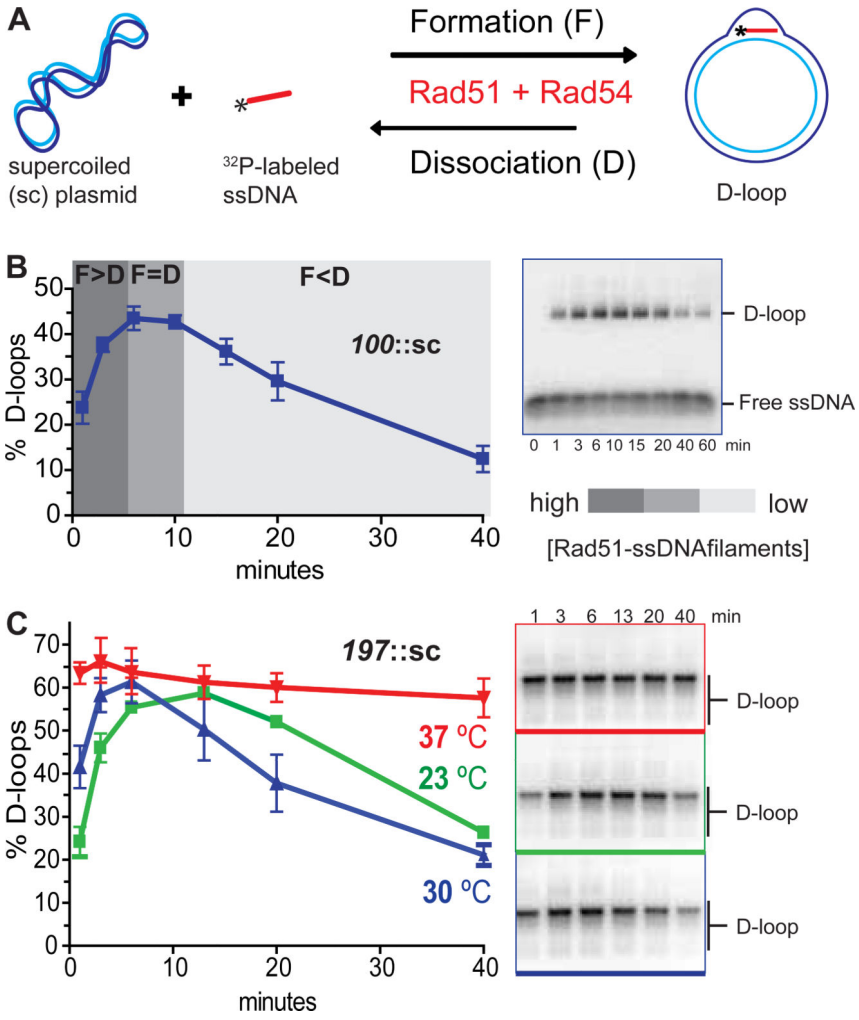

Figure 1. The D-loop cycle catalyzed by Rad51 and Rad54

A, Reaction scheme. **B**, Quantitation of D-loop reaction of a 100-mer paired with supercoiled plasmid DNA (denoted *100*::sc), with interpretation of net formation and dissociation phases of the reaction. A representative time course is shown. Here, and in all subsequent figures, unless stated otherwise: Reactions are at 30 °C; homologous ssDNA is present at 0.61 μM nt, donor dsDNA at 21 μM bp (3 kb, 7 nM molecules); Rad51 is saturating with respect to the invading ssDNA at 1 Rad51 to 3 nts ssDNA; RPA is at 1 heterotrimer to 25 nt ssDNA; Rad54 is at 84 nM monomers; Rad51 is added to ssDNA for 10 min, then RPA for 10 min, then Rad54 is added with the dsDNA. **C**, Reaction time courses of *197*::sc reactions. Rad51 filaments were allowed to form at 30 °C, then reactions were completed after dsDNA/Rad54 addition at 23, 30 or 37 °C (time '0' onward). Shown are means ± standard deviations of three or more reactions.

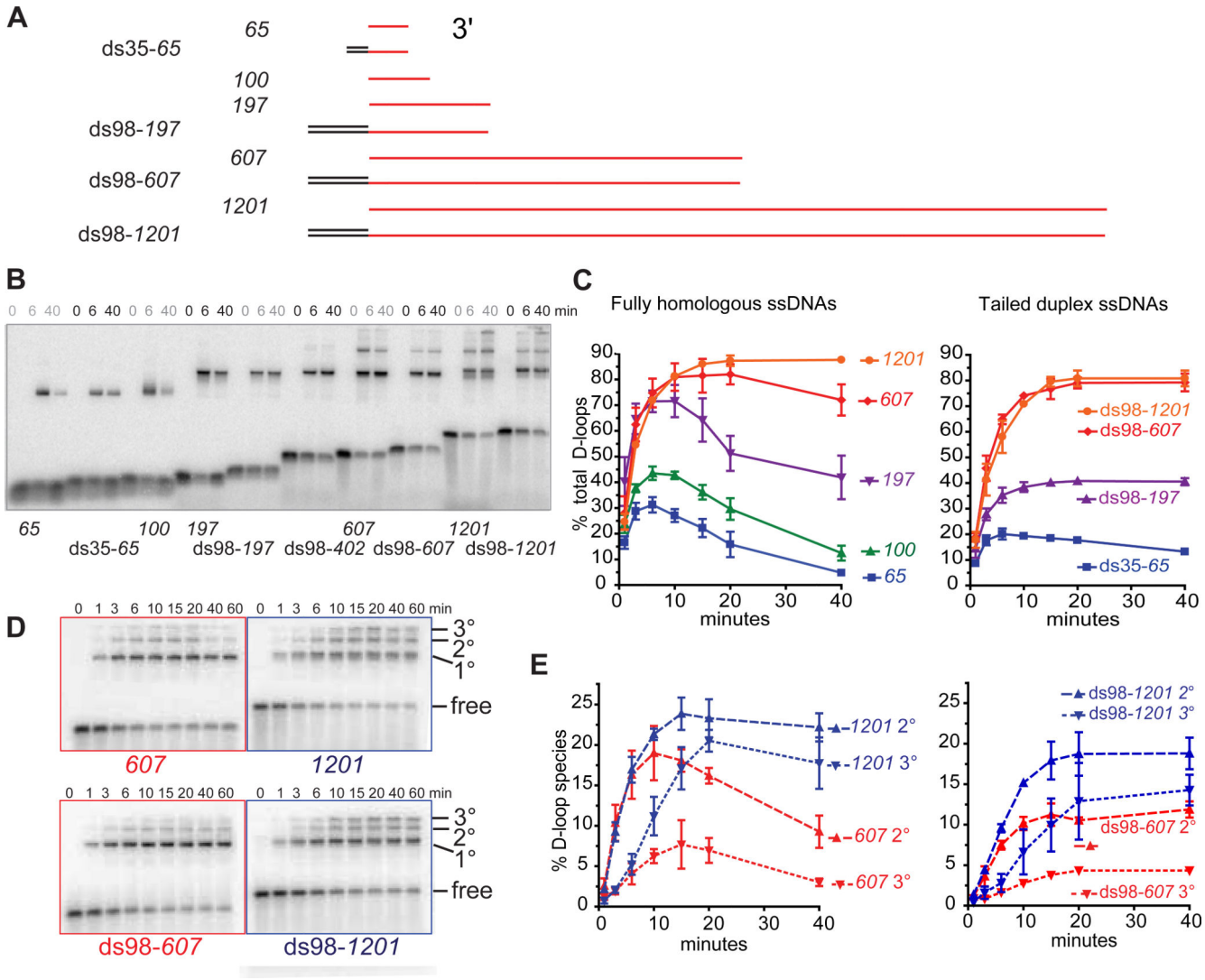

Figure 2. Physiological-length, tailed substrates form high levels of D-loops which are stable to dissociation

A, Scheme and nomenclature of substrates. **B**, Time courses of D-loop reactions with substrates shown in A paired with supercoiled plasmid DNA (0, 6, and 40 min time points). **C**, Quantitation of full D-loop time courses. Total D-loops are quantified, including single and MI species, if applicable. Fully single-stranded DNAs are plotted on the left and 5′-dsDNA-tailed DNA on the right. **D**, Time course gels (0, 1, 3, 6, 10, 15, 20, 40, and 60 min) showing the turnover of MI species. **E**, Quantitation of reactions shown in C. Shown are means ± standard deviations of three or more reactions.

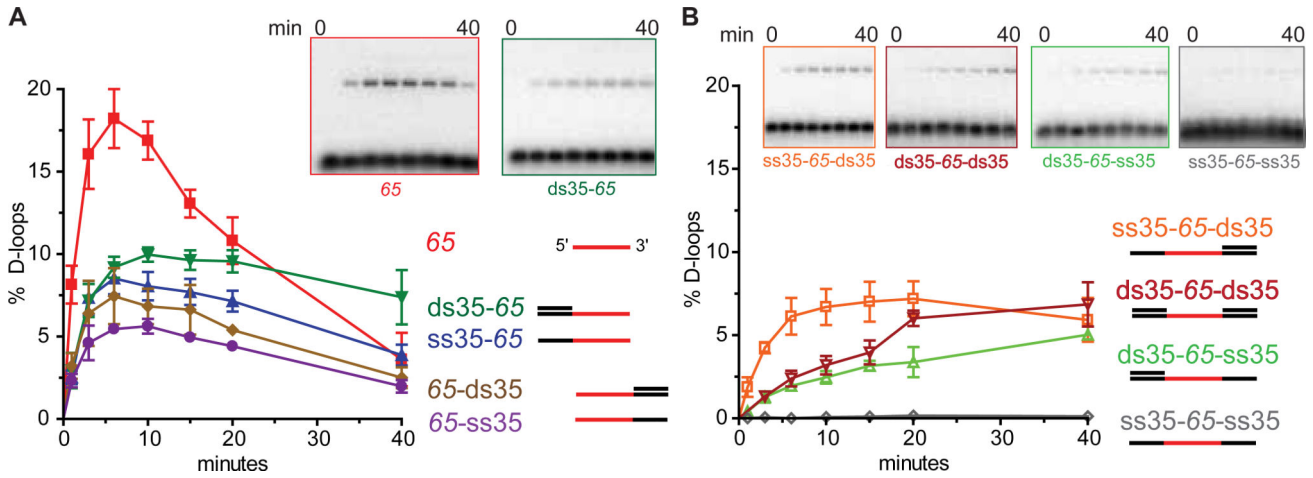

Figure 3. D-loops with short homologous ssDNAs are stabilized by heterologies flanking either side of the homology

D-loop reaction time courses of ssDNAs with 65 nt homology and the indicated heterologous double or single-stranded regions. The 65 nt homology substrates plotted on the left graph (**A**) have heterology on neither or one side of the homology, while those plotted on the right have heterologies on both sides (**B**). Shown are means ± standard deviations of three or more reactions.

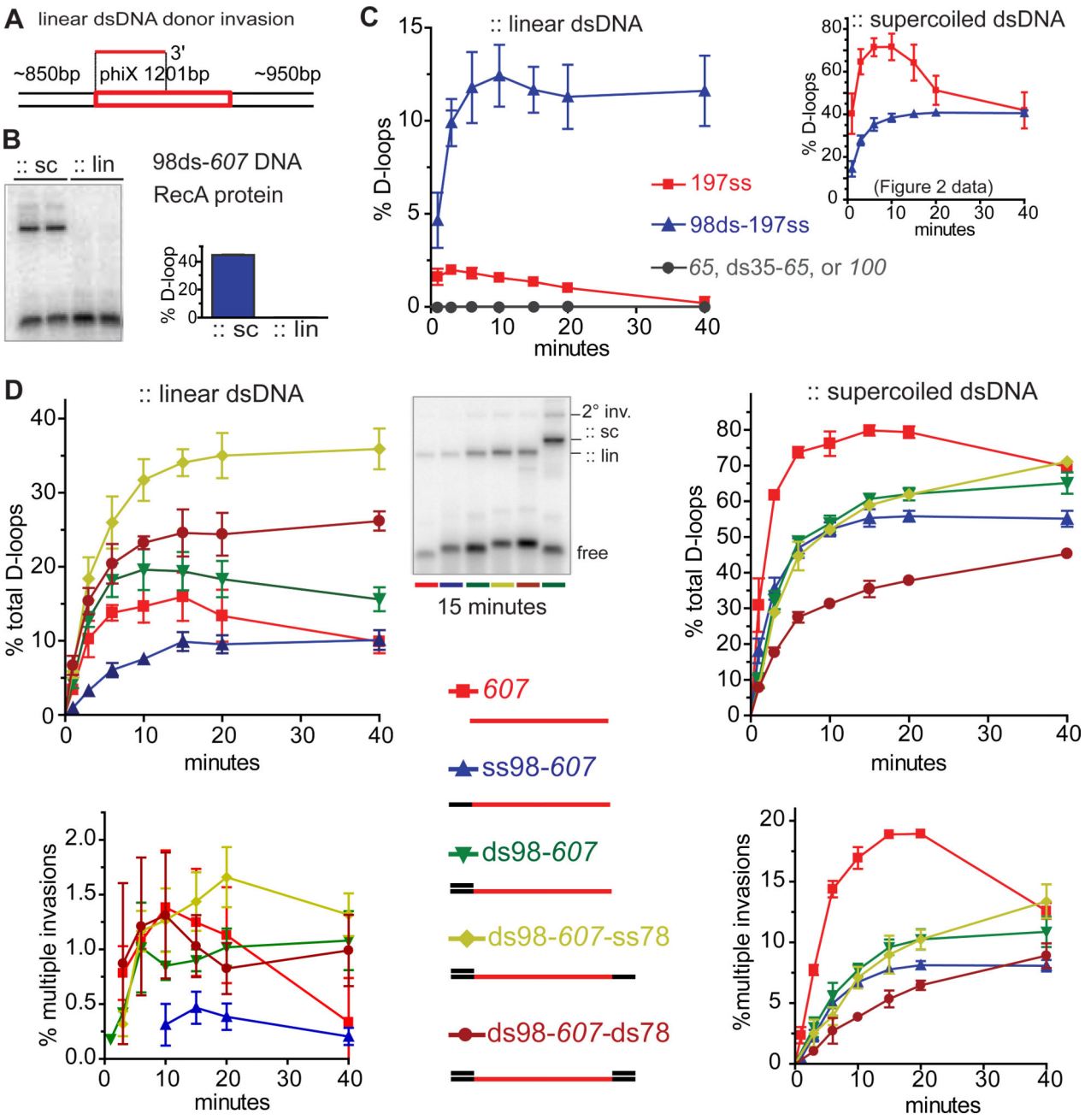

Figure 4. Rad51 and Rad54, unlike RecA, form D-loops with linear donor dsDNA

A, Schematic of the homology of the 607 nt invading ssDNA within the *Bsa*1-linearized dsDNA substrate. **B**, RecA protein D-loops, formed with supercoiled or linearized dsDNA (21 μM bps). **C**, Rad51/Rad54 *197* and ds98-*197* D-loops formed with linearized (left) or supercoiled (inset; same data as Figure 2B). **D**, Comparison of 607 nt homology substrates with 5′ or 3′ double or single-stranded heterologies. Linear donor reactions are plotted on the left (above, total D-loops; below, multiple invasions) and supercoiled reactions are plotted on the right. *Gel inset*: 15 min time point of linear dsDNA reactions. The last lane is a

control/migration marker ds98-*607*::sc reaction. Shown are means ± standard deviations of three or more reactions.

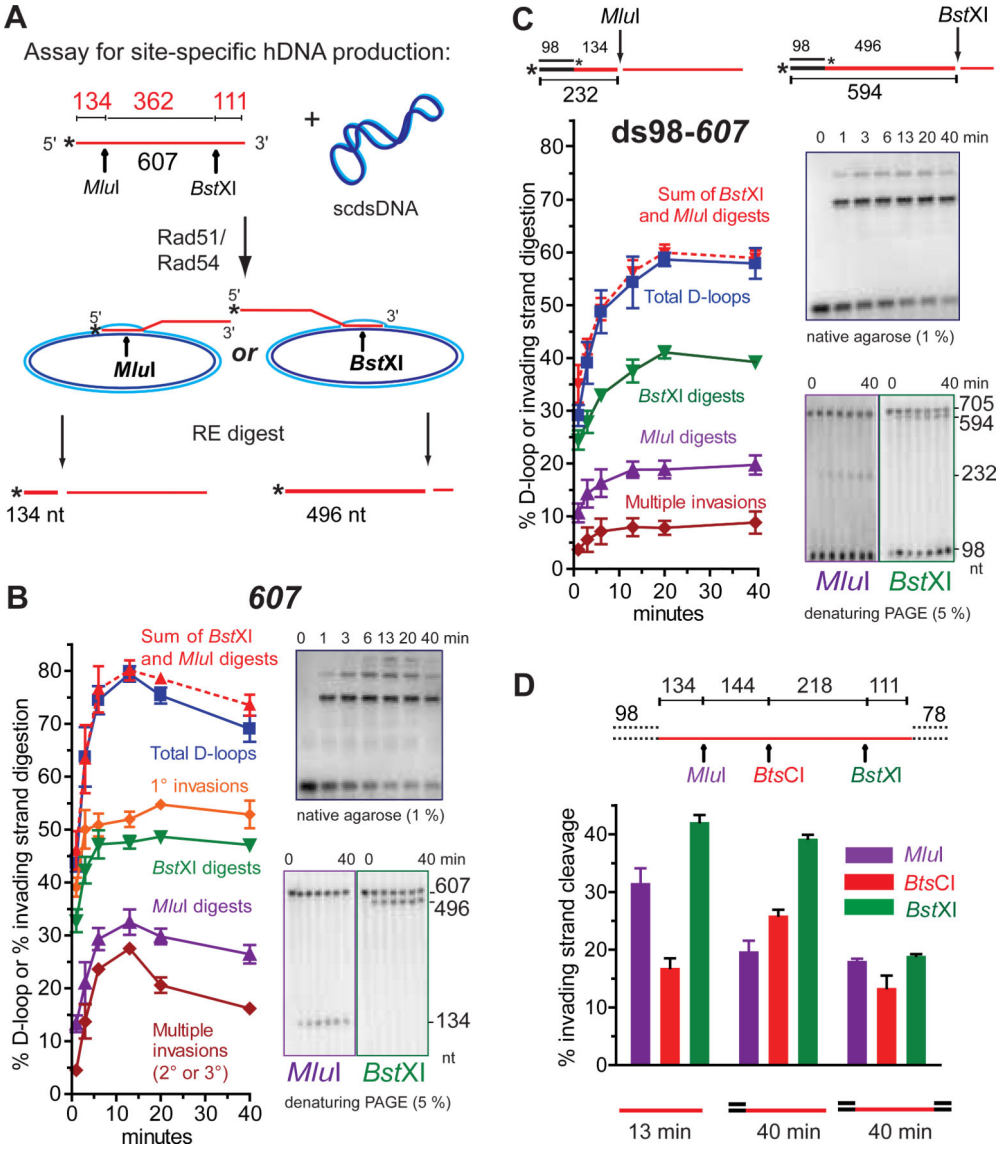

Figure 5. hDNA forms preferentially, but not obligatorily, at DNA ends with a modest preference for 3′ ssDNA ends

A, Scheme of the site-specific hDNA assay. **B**, *607*::sc and **C**, 98ds-*607*::sc D-loop reaction quantitations, with representative gels shown beside. The invading substrates used in C are shown. **D**, hDNA analysis of the indicated *607* homology substrates including an internal *Bts*CI site. Dotted lines indicate the optional dsDNA heterologies.

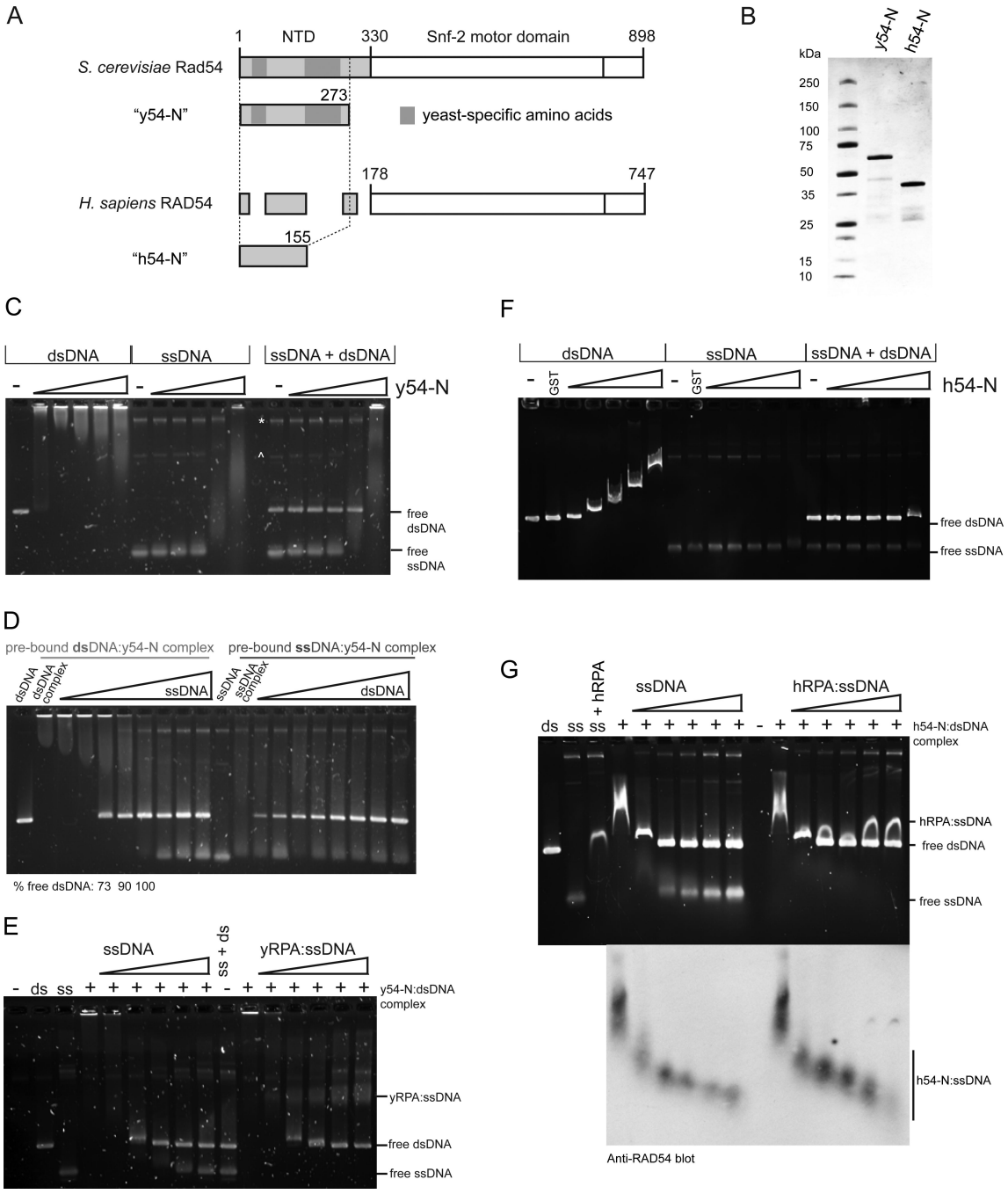

Figure 6. N-terminal fragments of yeast and human Rad54 preferentially bind ssDNA

A, Rad54 fragments cloned from yeast (y54-N) and human (h54-N) cDNAs contain the majority of the N-terminal domain. **B**, SDS-PAGE of purified GST fusions (2 μg) stained with coomassie blue. **C**, y54-N titration (0.6. 1.2, 2.3, 4.6, and 9.2 μM) on ssDNA (7.6 μM nt; ~ 3 kb, circular), dsDNA (7.6 μM bp; ~ 3 kb, linearized), and with ssDNA and dsDNA present (7.6 μM nt/bp each). The gel is stained with SYBR Gold. * and ^ mark minor dsDNA and ssDNA contaminants, respectively, in the ssDNA preparation. **D**, Pre-bound dsDNA or ssDNA y54-N complexes (7.6 μM nt/bp + 3 μM y54-N) were challenged by

titrating in the other DNA species (1, 2, 3, 4, 6, 8, 10, 15 μM bp or nt). **E**, Comparison of the ability of protein-free ssDNA *versus* yRPA-ssDNA to disrupt pre-formed dsDNA:y54-N complexes (7.6 μM nt/bp plus 3 μM y54-N). ssDNA concentrations are 2, 4, 6, 10 and 15 μM nt, and when present yRPA is at 1 heterotrimer to 25 nts (saturating). **F**, h54-N was titrated on the indicated DNA species as in C. The lanes marked "GST" contain 11 μM purified GST. **G**, Challenge of pre-formed dsDNA:h54-N complexes with ssDNA or hRPA:ssDNA as in E. The gel was stained with CYBR Gold (upper), and then transferred to PVDF membrane and probed with anti-hRAD54 antibody (lower).

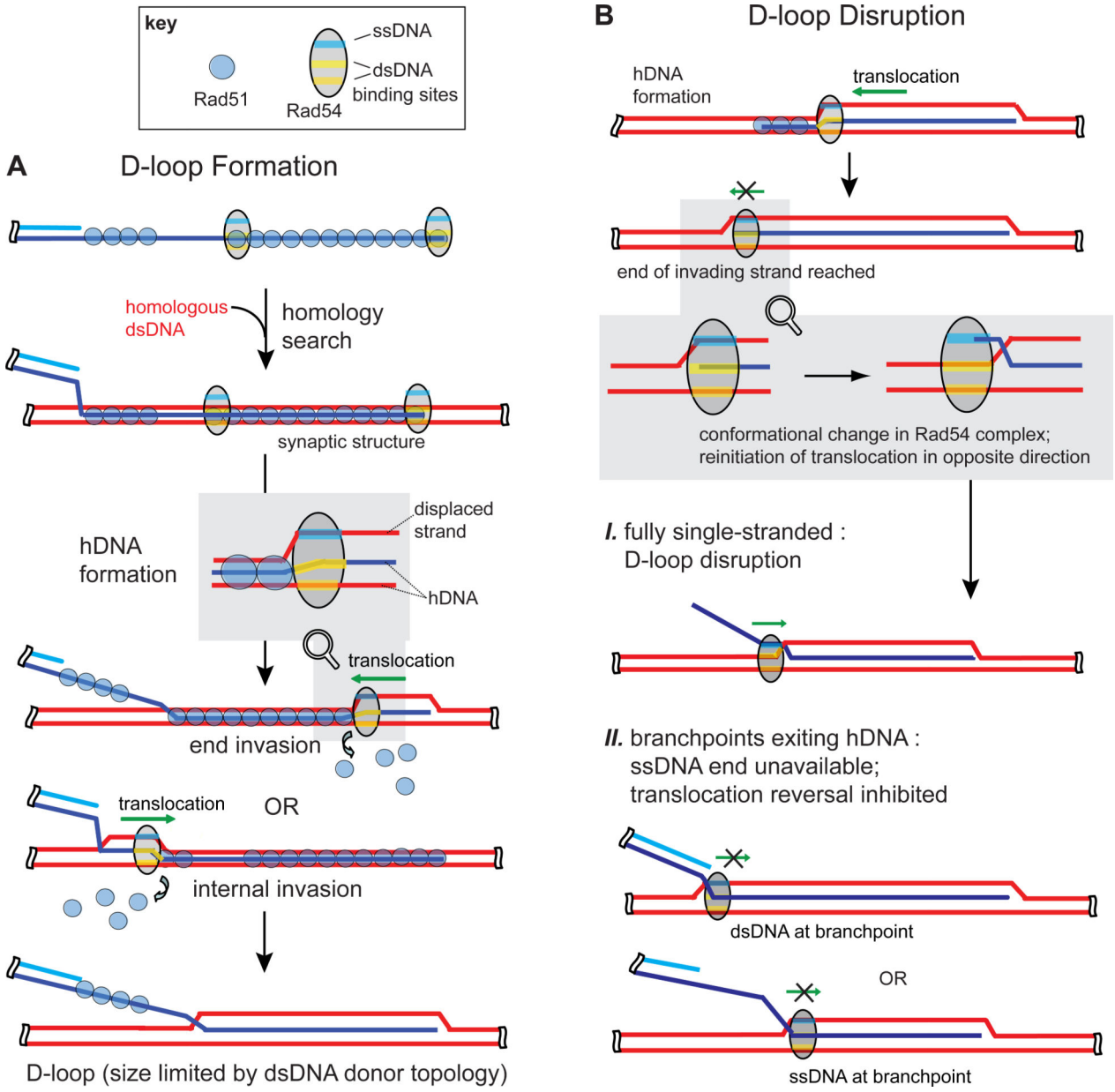

Figure 7. Heteroduplex DNA pump model for Rad54 function during HR. A, D-loop formation

The initial Rad51-mediated homologous joint DNA molecule is a three-stranded structure previously called a paranemic joint (Bianchi et al., 1983). Homologous base pairing occurs between the strands in some poorly understood fashion, but the invading strand is not yet in hDNA and the donor is no longer B-form dsDNA. To translocate, Rad54 requires dsDNA. A filament-terminal Rad51 monomer hands off the correct two DNA strands to Rad54, which begins to translocate on them, effectively pushing the two heteroduplex strands together ahead of itself to form the hDNA which it translocates upon. Rad51 filaments stimulate Rad54 translocation giving it directionality, resulting in the removal of Rad51 from the hDNA simultaneous with its creation. The displaced strand also stimulates Rad54 activity by binding the Rad54 N-terminal region, activating the Rad54 ATPase. **B, D-loop dissociation.**

Rad54, translocating on the two nascent hDNA strands, can only incorporate the invading strand into hDNA until it reaches the end of that strand. Single-molecule studies of Rad54 dsDNA translocation have shown complex behavior, such as pausing, reversing direction, and restarting at new translocation velocities, suggesting a change in the molecular species responsible for translocation (Amitani et al., 2006). At the D-loop, such a conformational change may involve switching the strands occupied by the core dsDNA binding (motor) domain and the N-terminal ssDNA binding domain (***case I***). Binding of the invading strand by the N-terminal domain orients the motor to translocate on two original dsDNA strands and displaces the original invading strand. The result is D-loop disruption by a similar mechanism as formation, but with different roles taken by the individual strands. We suggest that the proposed reversal in hDNA pumping, like hDNA formation, preferentially initiates from ssDNA ends, which are absent when branchpoints flank the hDNA region (***case II***). The greatest effect in stabilizing D-loops is imparted by terminal dsDNA (**Fig. 3**), which would not be bound productively by the N-terminal regulatory domain of Rad54 to promote D-loop disruption. Protein and DNA elements are not meant to represent actual structure or scale.